Effects of Autoclaving on the Ballistic Performance of Ultra High Molecular Weight Polyethylene Composites

by

Melissa Roth

A thesis submitted to the Faculty of the

WORCESTER POLYTECHNIC INSTITUTE

In partial fulfillment of the requirements for the

Degree of Master of Science

In

Materials Science and Engineering

May 2021

APPROVED:

_____

Dr. Brajendra Mishra, Advisor
Professor of Mechanical Engineering
Director, Manufacturing & Materials Engineering

ABSTRACT

Ultra high molecular weight polyethylene (UHMWPE) composites are becoming more frequently used in lightweight armor due to their low weight, high specific energy absorption, and high elastic wave velocity. These properties are due to the high crystallinity of the polymer chains, which are sensitive to processing conditions. To achieve good consolidation and matrix flow, the composites are initially pressed at pressures upwards of 24 MPa at elevated temperatures to allow for resin flow and consolidation. Some tensile strength of the fibers is lost during this process. If the composite is to be combined with another armor component such as a ceramic, it then goes through a second heat treatment in an autoclave so that it can be softened enough in order to shape it to the ceramic to obtain a good bond between the materials. Due to the proprietary nature of industry, UHMWPE composite processing methods, and resin content, little work has been published to quantify if and how the autoclaving process affects ballistic performance of composite armor systems. This study compared the mechanical properties of DSM Dyneema® HB210 (polyurethane matrix) and HB212 (styrene-isoprene-styrene (SIS) triblock copolymer matrix) composites before and after autoclaving by measuring composite density, t-peel strength, shear strength, tensile strength, flexural strength, and crystallinity. Ballistic performance of the composites was tested in a standalone configuration against 1.1 gram (17 grain) fragment simulating projectiles (FSPs) and in conjunction with a ceramic against a standard rifle threat. It was shown that autoclaving did affect the mechanical properties and fragment protection of the composites. Of note was an improvement in the resistance to fragment penetration for the HB212 following the autoclave procedure. When tested in conjunction with a ceramic, no change in performance was seen between the pre- and post- autoclaved samples.

ACKNOWLEDGEMENTS

This work was funded by the US Army Combat Capabilities Development Command Soldier Center (DEVCOM SC).

I would like to thank my teammates on the Ballistic and Blast Protection Team at DEVCOM SC for their help with equipment operation and discussion on this project. In particular, I am grateful to Jason Parker and Mike Maffeo for their valued input and feedback and to Rob DiLalla for supporting this endeavor.

Thank you also to my academic advisor, Dr. Brajendra Mishra, for the instrumental feedback on this paper and work herein.

CONTENTS

LIST OF FIGURES

LIST OF TABLES

1 INTRODUCTION

The traditional method for manufacturing small arms protective inserts (SAPIs) is to adhere an UHMWPE composite to a ceramic in an autoclave under heat and pressure. The composites are composed of 0°/90° UHMWPE fibers in a resin matrix of polyurethane (PU) or styrene-isoprene-styrene (SIS) triblock copolymer. These are layered and pressed under heat to consolidate into a curved SAPI shape. This annealing process leads to degradation of mechanical properties of the UHMWPE fibers.

This SAPI-shaped composite is then adhered to a curved ceramic. In order to achieve an even and consistent bond layer to the ceramic, it is necessary to reheat the consolidated composite in order to soften it and allow it to shape to the curved part without cracking the ceramic during cooling. It has been demonstrated by industry that this second heating can lead to further degradation but little has been published on this phenomenon as to the extent of its effect on ballistic performance.

2 MOTIVATION

The US Chief of Staff of the Army (CSA) has identified Soldier mobility as a priority for research and development. It is understood that weight has an impact on mobility and thus a reduction in body armor weight through the improvement of armor materials has been an area of interest to the Department of Defense (DoD) for many years. Combat Capabilities Development Command Soldier Center (DEVCOM SC) has headed multiple efforts on improving ballistic protection through the use of UHMWPE composites. The goal of these efforts was to understand how to utilize improved armor materials and minimize degradation during processing in order to reduce areal density of the armor without sacrificing area of coverage.

Further exploration into the mechanisms of mechanical property degradation during the autoclave process and its effect on ballistic performance in SAPI armor can allow for better

manufacturing and design of lightweight body armor while also providing a better understanding of the materials. This is especially important with the recent commercialization of novel UHMWPE composites from industry [1, 2]. It also has implications for material selection of adhesives and reinforcement materials used in SAPIs which may require the autoclave for curing at elevated temperatures.

3 OBJECTIVES

The objective of this research is to determine if the autoclaving process for bonding ceramic to UHMWPE armor results in further degradation of the UHMWPE composite and therefore reduces ballistic protection. Mechanical and ballistic properties of autoclaved and non-autoclaved UHMWPE were evaluated to determine if and how autoclaving during the armor production process is detrimental to armor performance.

4 LITERATURE REVIEW

Multiple efforts at the DEVCOM SC have been carried out to determine the best processing methods and materials for UHMWPE composite armor in head protection. Recent advancements in UHMWPE composites have led to the development of a lightweight helmet which offers a higher degree of protection than the currently fielded Army Combat Helmet (ACH) without added weight. The new UHMWPE composites produced by DSM and Honeywell have led industry armor manufacturers to further explore their uses in ceramic/UHMWPE torso armor. Due to the proprietary nature of armor manufacturing processes, little has been published on the specific processes, materials, and their effects on ballistic performance. More general research has focused on understanding how to enhance tensile strength of the PE fibers and failure mechanisms of composites.

4.1 MATERIALS

The materials used in personnel armor are UHMWPE resin-reinforced composites, selected for their high toughness and low weight. The composites are supplied as a unidirectional or 0°/90° prepreg reinforced with a matrix of either PU or SIS triblock copolymer matrix.

4.1.1 POLYETHYLENE

Ballistic performance of UHMWPE is due in part to the high crystallinity of the polymer chains. They are polymerized to molecular weights up to 10^7 Da and dispersed in a solvent, then gel-spun into long fibers and stretched to obtain a highly aligned orthorhombic crystal structure (>95% crystallinity). When extended, the chain will have weak van der Waals forces between hydrogen atoms in neighboring chains giving the fiber flexibility and strong C-C cohesive bonds within the chain leading to high strength on the order of 7 GPa and modulus of 235-325 GPa [7].

The drawn fibers are then coated by a low-melting-temperature thermoplastic with the purpose of maintaining alignment during consolidation. The material is supplied in 0°/90° or $(0°/90°)_2$ cross-ply sheets. The most commonly used materials are DSM Dyneema® and Honeywell Spectra Shield®.

4.1.2 MATRIX RESINS

The matrix resins used in both Dyneema® and Spectra Shield® are either PU- or SIS copolymer-based and typically at loadings of less than 20 wt%. The purpose of the matrix material is to protect the UHMWPE fibers and maintain alignment during consolidation and to transfer energy through the fibers during impact. In SAPIs, it also must provide structural support to the ceramic strike face to so that the ceramic interacts with the impacting projectile for as long as possible. The PU resins have a higher modulus than the SIS copolymer, which has more rubber-like properties. The PU matrix materials offer good support to a ceramic strike face in a SAPI and does not undergo as much delamination as the SIS copolymer matrixes which makes it ideal for helmet applications where large deformations are undesirable. SIS triblock copolymer resins are highly elastic and allow the fibers to elongate, becoming more resilient to fragments. They

deform more when impacted, leaving a large back face deformation (BFD) but effectively absorb impact energy through this failure mechanism. The resins are adjusted by the manufacturer to optimize for viscosity, fiber wetting, matrix volume content, elastic modulus, thermoformability, and other properties of interest.

4.1.3 CONSOLIDATION PROCESS

Sheets of aligned UHMWPE resin systems are consolidated into laminates in a 0°/90° orientation at approximately 140°C under pressure as described by the schematic in Figure 1 [3]. PE fibers are chemically inert, nonpolar, and have a low friction coefficient, making it difficult to consolidate them with a resin matrix. The elevated processing temperatures and high pressure are necessary for bringing the fibers into contact with the matrix to achieve van der Waals bonding between the materials.

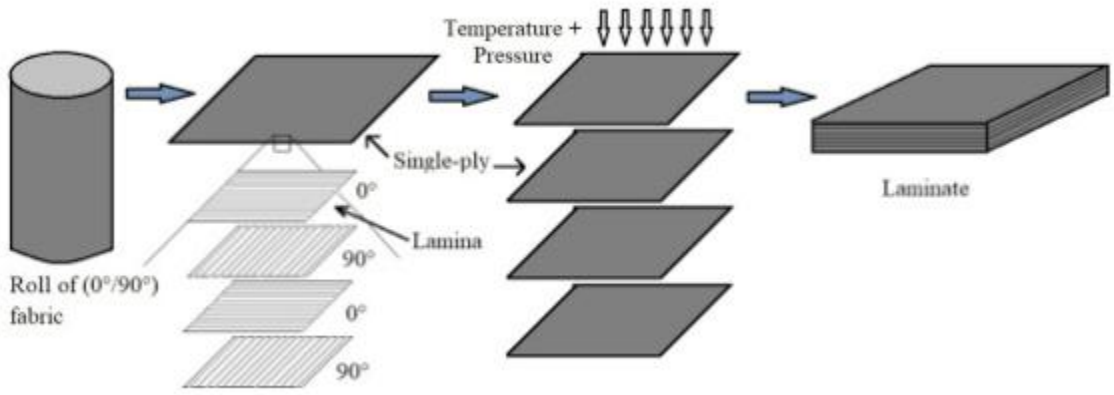

Figure 1 - A schematic of the fabrication process for a UHMWPE resin composite [28]

This process results in a composite laminate with good bulk properties, but up to 20% of the tensile strength of the fibers can be lost during processing at high pressures and temperatures due to annealing and thermal oxidative degradation. If the temperature is too high, degradation in the UHMWPE occurs in the form of chain breakage, branching, and cross-linking. If the temperature is too low, chemical reactions in the resin will not take place and this leads to poor interfacial adhesion between the fibers and resin matrix which in turn can lead to poor energy transfer along the fibers [4-6]. Despite processing difficulties, UHMWPE composites remain favorable as

compared to other composites such as aramids or fiberglass in personnel armor due to its light weight, high specific energy absorption, and high elastic wave velocity.

The resulting UHMWPE reinforced composite is highly anisotropic. The modulus in plane is orders of magnitude larger than the modulus through the thickness which is ideal for ballistic protection since the energy will more easily spread throughout the protective plate instead of through the plate towards the target [7].

For applications in SAPIs, the composite is paired with a ceramic strike face in a second manufacturing step. Both the composite and ceramic have a specified SAPI shape, but as shown in Figure 2 there is often some gap between the two parts due to shrinkage during manufacturing or slight differences in tooling between the composite and ceramic manufacturers.

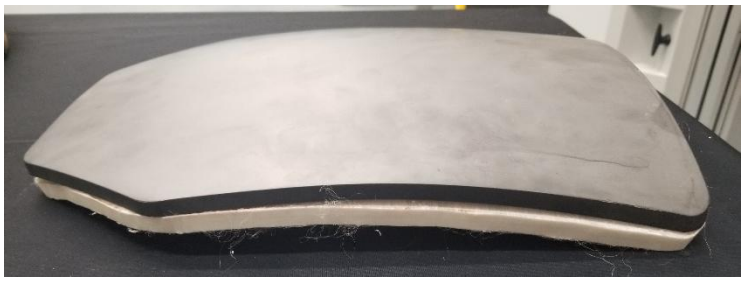

Figure 2 - A SAPI ceramic overlaying an UHMWPE composite before autoclaving

The purpose of the autoclave is to soften the consolidated composite enough at an elevated temperature and low pressure under vacuum so that it molds to the ceramic to form a uniform, even bond. The part is then cooled slowly under pressure so that the ceramic does not crack upon cooling due to the difference in coefficient of thermal expansion (CTE) between the two materials. Often there is an adhesive or reinforcement material between the ceramic and composite which may also need to be cured at a specific temperature.

4.2 FAILURE MECHANISMS

There have been advancements in UHMWPE composite armors in recent years due to incremental advancements in fiber strength [1, 2]. The goal of maximizing fiber strength for ballistic applications can be attributed partly to scaling analysis done by Cunniff which showed that the ballistic limit (V_{50}) of a material scales with fiber properties:

$$c = \left(\frac{\sigma_f}{\rho}\right)^{1/2} \left(\frac{\varepsilon_f}{4}\right)^{1/6} \quad \text{Eq. 1}$$

Eq. 1 gives the Cunniff V_{50} c in terms of the fiber ultimate tensile strength σ_f, fiber density ρ, and fiber ultimate tensile strain ε_f [8]. A high tensile strength resists stretching forces during fiber deflection and a high ultimate tensile strain aids in converting the kinetic energy of debris from the ballistic impact to potential energy during fiber fracture [8]. A low density is desirable for lightweight armor applications.

The goal of maximizing fiber strength and minimizing annealing during UHMWPE composite processing has been the subject of many studies [4, 9-12]. To minimize voids which introduce localized stresses in the composite, the laminates are heated to obtain good wetting and resin flow. During this unconstrained heating period, the fibers relax and in the process lose mechanical strength. For this reason, it is predicted that a second heating step using an autoclave would further degrade the fibers if not properly constrained. However, Cunniff's work does not take into account the matrix properties, the fiber density within the laminate, or the influence of failure strain. It was also based on the assumption that projectiles do not deform. This model was appropriate for fabric-based armors but does not give a full and accurate description of a composite system. A study later done by Lee et al. showed that even at very low resin loadings the matrix properties had an impact on ballistic limit [3].

More recent work by Karthekeyan et al. has explored how laminate properties contribute to the failure of materials at high strain rates [5, 13]. They identify three mechanisms of laminate deformation:

1. Fiber fracture –Fibers in the 90° direction are restrained by fibers in the 0° direction, leading to a buildup of compressive stress in the 90° and tension in the 0° direction until tensile fiber failure occurs. Fiber misalignment or waviness due to fiber relaxation during processing will lead to uneven loading and can cause some fibers to prematurely fail, lowering the strength of the material [8].
2. Friction – Energy loss to friction occurs during fiber pull-in, along the delamination plane, and between the projectile and laminate.
3. Matrix shear – Interlaminar shear occurs between plies and intralaminar shear occurs between fibers within a ply.

When a composite is impacted by a projectile, it sends wavelets in the primary fibers directly beneath it out longitudinally with a propagation velocity of c_L [8], traveling ahead of the projectile. This deflection in the primary fibers causes straining and transverse motion of the secondary fibers, those not in contact with the projectile. In this first section directly beneath the projectile, fiber fracture is the main mechanism of energy absorption and no delamination is seen. The layers below this delaminate in failure modes I and II [2, 14]. Typically, the magnitude of the stress wave caused by a ballistic impact is greater than that of the yield stress of the armor material, leading to a wave consisting of plastic and elastic parts. The velocity of the elastic wave is determined by the Young's modulus and material density [14, 16] and the state change from state 0 to 1 in a material can be described by the Rankine-Hugoniot equations:

$$\rho_1 u_{P1} = \rho_0 u_{P0} \qquad \text{Eq. 2}$$

$$P_1 + \rho_1 u_{P1} = P_0 + \rho_0 u_{P0} \qquad \text{Eq. 3}$$

$$e_1 + \frac{P_1}{\rho_1} + \frac{{u_1}^2}{2} = e_0 + \frac{P_0}{\rho_0} + \frac{{u_0}^2}{2} \qquad \text{Eq. 4}$$

where ρ is the material density, u is the particle velocity, e is the internal energy, and P is the pressure for the state change. The magnitude of the strain wave velocity is proportional to $\sqrt{E/\rho}$ where E is the elastic modulus of the composite and ρ is the composite density.

When the wave reaches an interface such as the ceramic-composite interface in armor, a stress wave is reflected back into the ceramic. The magnitude of this wave will be determined by the impedance of the two materials, thus it is important to know the properties of the bulk composite when designing armor. One such study showed that consolidation pressure affected ballistic resistance and shockwave behavior [7]. At particle velocities u_P below 1100 m/s, shock speed velocity and V_{50} increases with consolidation pressure [7].

It should also be noted that these failure mechanisms outlined by Karthekeyan do not occur throughout the thickness of the target. The strike face layers fail by fiber fracture and failure mode then changes to fiber pullout and delamination in the layers that remain unbroken [10]. This change in failure mode implies that delamination and therefore interfacial properties affect ballistic performance.

While Cunniff's work and other studies [17] have shown that fiber strength dominates the ballistic performance response, it is important to understand how the matrix plays a role in other failure mechanisms. The relationship between composite shear strength and ballistic performance cannot be captured by predictions made by Cunniff's scaling work.

4.3 PHYSICAL, MECHANICAL, AND BALLISTIC PROPERTIES OF UHMWPE COMPOSITES

While ballistic tests are the final stage for determining the efficacy of body armor, lab scale test methods are used to characterize the properties of ballistic materials for modeling purposes and to understand which properties can be linked to ballistic performance. In addition to linking the mechanical properties to ballistic performance, there have also been many studies on how processing conditions affect these properties of UHMWPE composites in order to optimize the material for various applications [4, 9-12, 18, 20-24]. In each case it was concluded that UHMWPE composites are sensitive to temperature and/or pressure conditions. It was based on these studies that the test methods and materials for the following work were selected.

4.3.1 DENSITY

Density of the UHMWPE composites is of interest because it is an indication of void formation or a change in crystallinity during processing. Voids weaken the matrix by inducing localized stresses and decreasing energy dissipation. A higher density correlating with low porosity has been shown to increase shock wave speed during ballistic impacts [24]. The shock wave transmitted back to the ceramic will determine the extent of the damage to the ceramic. A highly cracked or fragmented ceramic will not protect against a second impact and some of the fractured mass will be transferred into the composite, leading to deformation.

Xu and Harris showed that density of a Spectra Shield UHMWPE composite increased with processing temperature up to 154°C due to lateral deformation of the fibers filling in interstitial gaps in the lamina. At higher temperatures, the density decreased due to excessive melting of the crystalline phase which cools into a less-dense amorphous phase. They also noted that at high processing pressures, pressure-induced crystallization may occur, wherein fibers are forced to orient into a crystal structure under pressure [23].

4.3.2 TENSILE STRENGTH

Tensile tests comparing pristine, unconsolidated DSM Dyneema® HB210 $(0°/90°)_2$ sheets with consolidated sheets showed a reduction in tensile strength [9]. This can be attributed to the aforementioned annealing of the fibers which induces a waviness to the structure through the loss of crystallinity. This waviness causes non-uniform loading of the constituent fibers leading to fiber failure. It is therefore important to understand how processing at elevated temperatures affects the properties of the fiber to avoid further degradation.

As shown by Cunniff, a high fiber strength is necessary for good ballistic performance and has been shown to dominate ballistic performance in composites and fabrics [8]. This primary failure mechanism of fiber fracture occurs in the top region of the impacted target.

4.3.3 T-PEEL

T-peel strength can be used as an indication of adhesion strength between plies of material. Good adhesion is necessary for stress transfer between fibers and matrix and contributes to lateral strength [23]. In this test, two plies are peeled apart and the force vs displacement is measured. It is expected that the peel strength is stronger for composites where more melting and recrystallization upon cooling has taken place since there would be better bonding. Better adhesion leads to a higher lateral strength, but at the expense of longitudinal strength. Adhesion should be high enough to effectively dissipate energy along the fibers but should not impede delamination [23].

Tailoring interfacial adhesion for UHMWPE composites is difficult due to their inert structure and lack of side chains. Bonding a matrix to the fibers often requires some treatment step which will degrade the fiber properties [25]. However, the use of a thermosetting resin with better UHMWPE fiber compatibility which can be cured in an autoclave curing cycle could allow for the development of new resins if it can be shown that autoclaving does not degrade the fibers.

4.3.4 SHEAR STRENGTH

Three- and four-point bend methods can be used to measure the flexural properties of laminates. Studies have shown that a high fiber strength in combination with low interlaminar shear strength (ILSS) was beneficial for ballistic applications because the interlaminar shear alleviates buildup of bending stresses through the beam thickness and matrix yielding protects the fibers from bending stresses [5, 9, 10, 13, 14, 26].

ILSS will affect the delamination between plies, one of the mechanisms of energy absorption that will depend on the bulk properties of the composite [4, 5, 9, 17]. While a low shear strength is desirable for protecting fibers from the buildup of stresses, if it is too low then delamination can occur early in the composite. This will prevent it from supporting the ceramic and can lead to a decrease in ballistic performance when used in a ceramic/UHMWPE composite armor system [14]. Karthekeyan's work showed that ballistic limit correlates inversely with shear strength, and this was confirmed by DEVCOM work [5, 9].

As previously noted, the square root of the flexural strength or modulus is proportional to the speed of the strain wave propagation during an impact event. A higher in plane modulus is desirable for spreading energy throughout the composite instead of through the thickness of it [26].

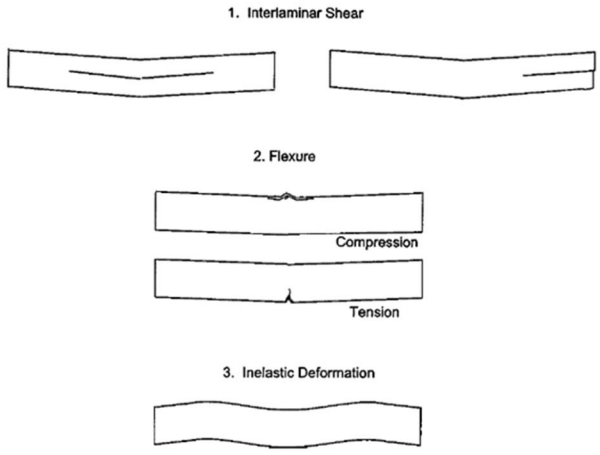

Figure 3 - Failure mechanisms for shear beam testing [27]

Figure 3 shows the failure mechanisms induced by bend tests. UHMWPE composites typically deform by interlaminar shear and inelastic deformation due to their flexible nature. These can be seen both in low strain rate bend tests and in high strain rate ballistic tests.

4.3.5 DSC

Differential scanning calorimetry (DSC) was used to observe the thermal properties of HB210 and HB212 and determine the degree of crystallinity in the processed samples. Maintaining a high degree of crystallinity in the UHMWPE fibers is important in maintaining fiber strength. Enthalpy of melting (ΔH_m) and enthalpy of recrystallization (ΔH_c) are calculated by integrating the melting peaks during heating cycles and recrystallization peak during the cooling step, respectively. The percent crystallization is calculated using Eq. 5, where X_C is percent crystallinity, ΔH_m is the enthalpy of melting as measured by DSC, and $\Delta H_m°$ is the enthalpy of melting for pure crystalline PE (293 J/g).

$$X_C = \frac{\Delta H_m}{\Delta H_m^\circ} \times 100\% \quad \text{Eq. 5}$$

In addition to quantifying crystallinity, DSC can indicate the type of crystal structure present in the UHMWPE. A large endotherm in the first heat cycle represents the melting of the orthorhombic crystals. At several degrees higher, samples may show another smaller endotherm corresponding to the melting of hexagonal crystals [4, 22]. The presence of hexagonal crystals is indicative of pressure induced crystallization during the consolidation process. The more mobile hexagonal phase causes the stresses in the fibers to relax, leading to a decrease in tensile strength [22].

4.3.6 BALLISTIC LIMIT, V_{50}

The ballistic limit, or V_{50}, is the velocity at which a specified projectile has a 50% chance of penetrating a particular armor. It is often used as a protection criteria and performance standard for armor performance. The value is specific to a projectile and armor system and is calculated by averaging equal numbers of the highest velocities for partial penetrations and lowest velocities of complete penetrations. A partial penetration is defined as an impact where the projectile does not penetrate the final layer of the target and a complete penetration is when the projectile passes through the target. The V_{50} is a standard of protection used in performance specifications for armor and is therefore what ultimately determines the pass/go criteria for a material. However, ballistic tests for research and development purposes are time, cost, and

material prohibitive and so researchers are often looking to relate other mechanical and physical properties to ballistic performance or use the properties to create a reliable constitutive model.

Of interest for this project are fragment simulating projectiles (FSPs) and rifle threats. FSPs are laboratory test projectiles designed to simulate irregularly shaped fragments from bursting munitions, traveling at 300-1000 m/s in an array of sizes. The FSPs are comprised of hardened steel and have a beveled nose as shown in Figure 4. A 1.1 g (17 gr) 0.22 cal FSP was selected for this study.

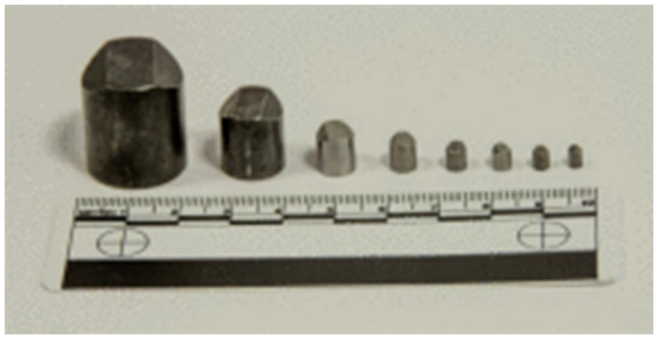

Figure 4 - FSPs used for ballistic testing [25]

A rifle round was selected based on SAPI protection requirements. These threats range from 0.215 cal to 0.308 cal in diameter and unlike the FSPs have a pointed tip. Some have a lead or mild steel core while others contain a hardened steel or tungsten core. These threats can travel at velocities of roughly 910 m/s. A ceramic strikeface is required to blunt the incoming projectile and the UHMWPE composite backing supports the ceramic and stops the remaining pieces of projectile.

Though not studied as part of this effort, BFD is also a metric of interest when evaluating ballistic materials and is heavily dependent on interlaminar strength. BFD is the deformation that occurs on the back of the target after penetration. It is measured by impacting targets at the V_0 velocity (the projectile velocity at which no penetrations will occur) and averaging the distance between the target and rear of the deformed sample. It is caused by delamination and stretching of the material. A large BFD can injure the user and thus there is a trade space for good energy absorption through deformation while minimizing the size of the BFD to minimize injury. It has

been shown that PU-based composites exhibit lower BFD measurements by as much as 45% as compared to SIS copolymers [5].

5 EXPERIMENTAL METHODS

5.1 MATERIALS

DSM Dyneema® HB210 and HB212 were selected as the backing materials. They have the same areal density and fiber type (Dyneema SK99) but with differing resin systems: HB210 has a polyurethane-based resin matrix and HB212 has a SIS triblock copolymer resin matrix. Both have a single-ply thickness of 140 μm and come in a $(0°/90°)_2$ sheet of cross plied unidirectional fibers pre-impregnated with the matrix.

CoorsTek® UltraSiC™ SC30 ceramic was used as a strike face for samples tested against a rifle threat. This is a sintered silicon carbide (SiC) ceramic often used in hard armor. These flat tiles were 10.16 cm x 10.16 cm square with a density of 3.15 g/cm^3 and average thickness of 0.89 cm.

Sika® Sikaflex®-252 is a polyurethane adhesive used to adhere the ceramic to the Dyneema composites for ballistic testing. This adhesive air-cures with exposure to moisture.

5.2 EQUIPMENT

Hydraulic press, 392 ton capacity with 50 cm ram

Instron® Universal Testing System 5500R with 1kN load cell

Instron® Universal Testing System 5969 with 10kN load cell

TA Instruments DSC Q100 differential scanning calorimeter

ASC Process Systems autoclave

5.3 SAMPLE PREPARATION

UHMWPE composite backings with an areal density of 4.9 kg/m^2 were prepared using a hydraulic press. Material was cut to 38 cm x 38 cm and 36 sheets were stacked in a 0°/90° fiber orientation for a total of 72 0°/90° layers. The layups were placed between sheets of fiberglass-reinforced Teflon® which were then placed between 38 cm x 38 cm aluminum caul plates as shown in Figure 5. This was placed between the pre-heated platens of the press at 140°C and allowed to come up to temperature under no pressure for ten minutes. The samples were then pressed at temperature for 20 minutes at 24 MPa. After 20 minutes, the samples were cooled under pressure to room temperature at a rate of roughly 1°C/min.

Figure 5 - A schematic of a composite layup for flat UHMWPE test panels

Tensile test samples were prepared by pressing a single sheet at the same processing parameters as the plates and then cut to 23 cm long by 1.3 cm wide.

T-peel samples were prepared by consolidating two sheets at the same processing parameters as the plates leaving 76 mm unbonded as shown in Figure 6. Samples were then cut to 25 mm wide as specified by ASTM D1876-08 [29].

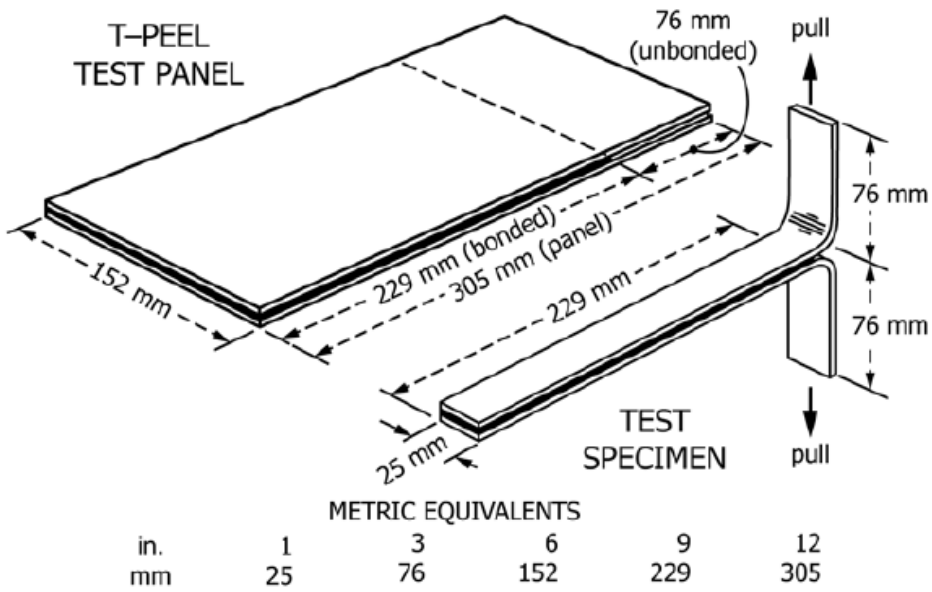

Figure 6 - Schematic of a t-peel test specimen [29]

The three- and four-point beam samples were prepared by cutting the 4.9 kg/m^2 plates to the appropriate sizes specified in the ASTM methods using a band saw. Three-point samples were cut to a length-to-thickness ratio of 6:1 and a width-to-thickness ratio of 2:1 as specified by ASTM D2344 [27]. The three-point bend samples were also used for density measurements. Four-point beam samples were cut to a length of 90 mm and width of 10 mm as specified by ASTM D7264 [30].

DSC samples were prepared by cutting single plies of processed material left over from tensile test strip samples into 5-8 mg pieces. These were hermetically sealed inside a DSC sample cup for testing.

Non-autoclaved ceramic composite armor was prepared by adhering a 10.16 cm x 10.16 cm ceramic tile to the surface of a consolidated UHMWPE backing and allowing the adhesive to cure at room temperature. The 38 cm x 38 cm panels were cut into quarters and a ceramic tile was centered on each square as shown in Figure 7. The ceramics were adhered by spreading a

layer of Sikaflex®-252 over the back and placing eight 2.5 cm pieces of 0.49 mm monofilament wire over the adhesive layer in order to ensure an even bond line. The ceramic was placed on the backing and placed in a vacuum bag for a minimum of 4 hours to obtain good contact between the ceramic and composite.

Autoclaved samples were placed in the vacuum bag inside the autoclave. For the samples with ceramics this was done within 1 hour of applying the Sikaflex®-252 adhesive and assembling the armor. After pulling a vacuum, the temperature was raised to 93°C at a rate of 5°C/min. The temperature was held for 5 min and then the pressure inside the autoclave was increased to 0.69 MPa. The sample was held at this temperature and pressure for 20 min and then temperature was decreased to 27°C while under pressure. The pressure and vacuum were then released before sample removal.

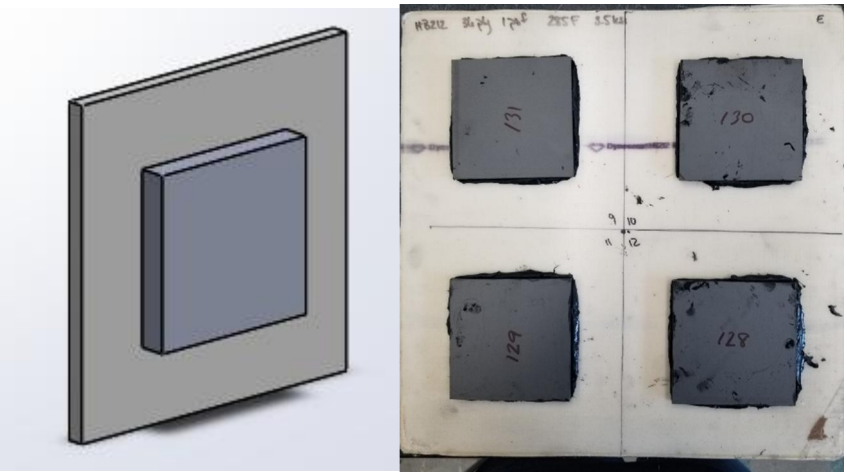

Figure 7 - Ceramic tiles adhered to a UHMWPE composite backing using Sikaflex-252 adhesive

5.4 TEST METHODOLOGY

5.4.1 DENSITY

Density was measured using the Archimedes method according to ASTM D792-13 [31]. Composite samples prepared for three-point bend tests were used as samples specimens. For each specimen, the mass of the sample in air (*a*) was measured. The sample was then suspended from a metal sinker in water and the mass of the sinker and sample (*b*) was measured. Lastly, the

sample was removed and the mass of the sinker in water (*w*) was recorded. The specific gravity was calculated using Eq. 6:

$$sp\ gr\ \frac{23}{23}℃ = a/(a + w - b) \qquad \text{Eq. 6}$$

Five specimen per sample were tested.

5.4.2 TENSILE TESTS

The Instron® 5969 universal testing system (UTS) was used to measure load vs. extension. Strips were clamped at 620 kPa with a gauge length of 10 cm. The top crosshead was moved up at a rate of 50 cm/min until specimen failure. Twenty specimen per sample were tested.

5.4.3 T-PEEL TESTS

The standard test method for Peel Resistance of Adhesives (ASTM D1876-08) was used to determine the t-peel loadings over a 6" length of the sample. The unbonded ends were clamped at 620 kPa with a gauge length of 5 cm. The top crosshead of the UTS was moved up at a rate of 254 mm/min for a total length of 305 mm. The tensile load was measured as a function of displacement. Ten specimen per sample were tested.

5.4.4 SHORT BEAM SHEAR STRENGTH

Short beam shear strength was measured according to ASTM D2344 [27]. The Instron® 5500R UTS was equipped with a flex fixture and shear head as shown in Figure 8. The span of the flex fixture was set such that the span-to-thickness ratio was 4:1.

Figure 8 - The Instron® UTS with three point bend fixture

The top crosshead was moved down at a rate of 1 mm/min and load was measured as a function of displacement until the load dropped by 30%, signaling the end of the test. The shear strength was calculated using Eq. 7, where P_m is the maximum load recorded, b is the specimen width, and h is the specimen thickness.

$$F^{sbs} = 0.75 \times \frac{P_m}{b \times h} \qquad \text{Eq. 7}$$

Ten specimen per sample were tested.

5.4.5 FLEXURAL STRENGTH

Flexural strength of composites was measured according to Procedure B of ASTM 7264 [30]. The Instron® 5500R UTS was equipped with a four-point bend fixture with a base span of 80 mm and a load span of 40 mm. The load span was moved down at a rate of 0.018 mm/s to obtain a strain rate of 10^{-4-} s^{-1} and stress was measured as a function of displacement. Flexural strength S of the composites was calculated using Eq. 8, where P is the maximum force, L is the specimen length, b is the specimen width, and d is the specimen thickness.

$$S = \frac{3PL}{4bd^2} \qquad \text{Eq. 8}$$

Ten specimen per sample were tested.

5.4.6 DIFFERENTIAL SCANNING CALORIMETRY

DSC was performed using a TA Instruments DSC Q100. Samples 8-12 mg in weight were hermetically sealed in aluminum pans. Samples were held at 20°C for two minutes then ramped to 200°C at a rate of 10°C/min. Samples were then cooled to 20°C at a rate of 10°C/min before heating a second time to 200°C at 10°C/min.

5.4.7 BALLISTIC LIMIT, V_{50} TESTS

V_{50} values were obtained for 4.9 kg/m^2 flat panels for 17 gr FSPs and for the ceramic-fronted panels against a rifle projectile. FSP tests were performed at DEVCOM SC using a helium gas gun and rifle round tests were conducted at NTS Chesapeake (Belcamp, MD). The V_{50} was calculated using regression analysis.

6 RESULTS AND DISCUSSION

6.1.1 DENSITY

Density measurements for composites before and after autoclaving are shown in Figure 9. A t-test showed that the increase in density due to autoclaving for HB212 was not statistically significant ($p>0.05$), but a decrease in void content can be seen in computed tomography (CT) scans taken by NTS Chesapeake.

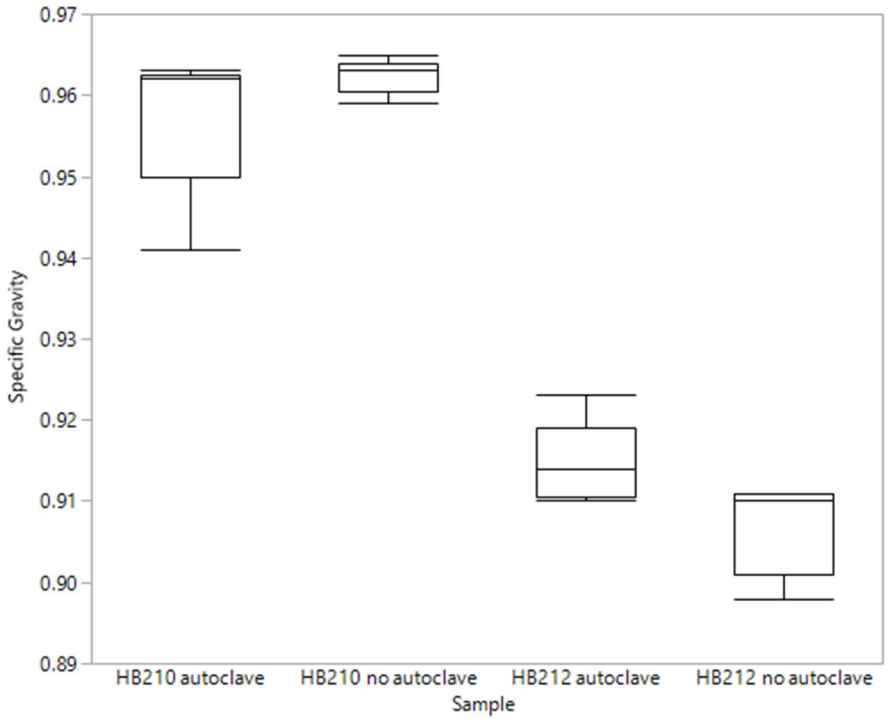

Figure 9 - Density of HB210 and HB212 before and after autoclaving

CT scans of the pre- and post-autoclaved samples are shown in Figure 10. The red and blue regions indicate the presence of voids. The HB212 sample has significantly fewer areas of poor lamination after autoclaving. Of the two materials, HB212 has the less viscous resin which will more easily flow during the autoclaving process leading to a decrease in porosity.

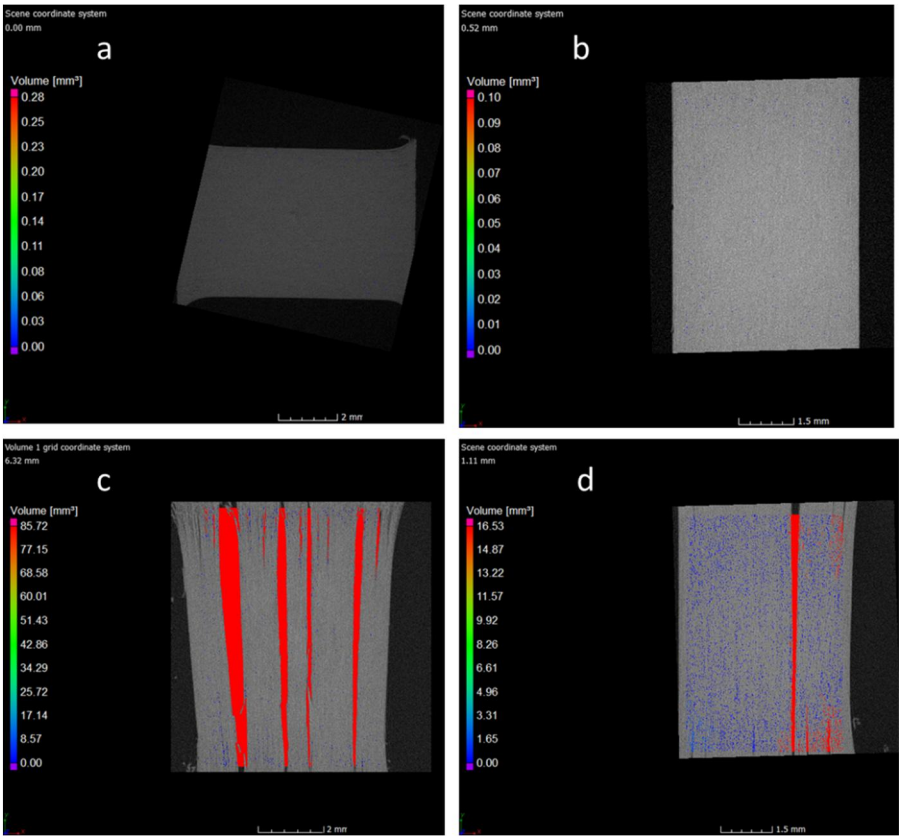

Figure 10 - CT scans of HB210 (a) before autoclaving and (b) after autoclaving HB212 (c) before autoclaving and (d) after autoclaving

6.1.2 TENSILE STRENGTH

Maximizing the tensile strength of the UHMWPE fibers has been the industry goal when making commercial ballistic composites. The tensile test is a measurement of the longitudinal strength of these fibers in one direction. The HB210 and HB212 have the same fiber type (Dyneema SK99) and should therefore have the same tensile strength for this test where matrix strength is negligible. Figure 11 shows the ultimate tensile strength of the HB210 and HB212 before and after autoclaving.

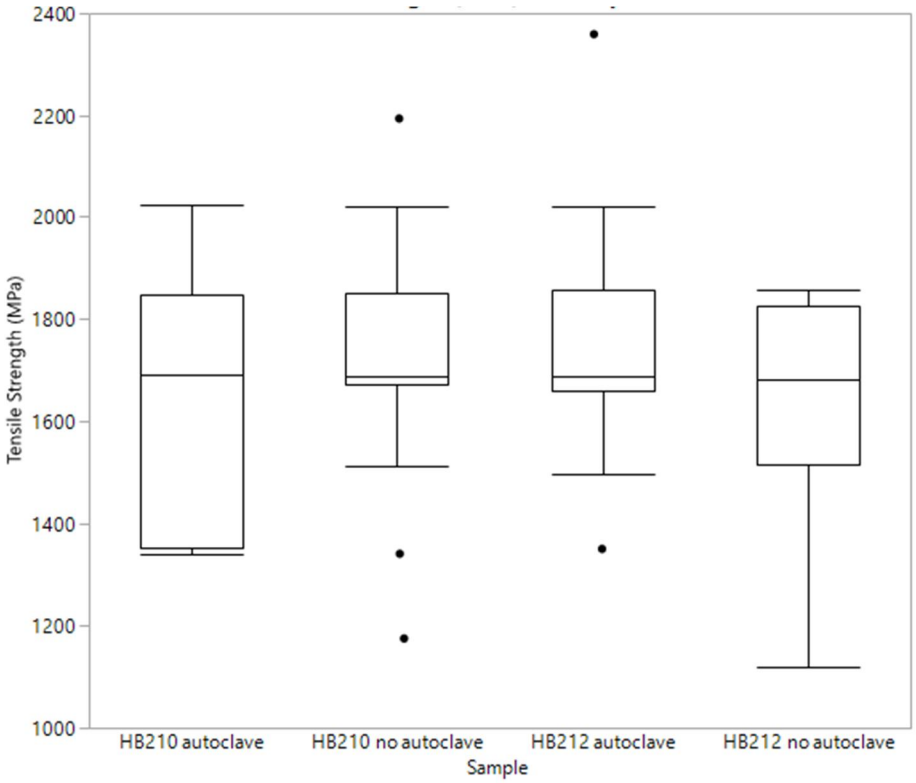

Figure 11 - Ultimate tensile strength of HB210 and HB212 before and after autoclaving

A t-test showed that there were no statistically significant ($p>0.05$) changes in tensile strength due to autoclaving for either the HB210 or HB212. This suggests that any change in performance can be attributed to changes in the material bulk properties and not to damage to the UHMWPE fibers.

6.1.3 T-PEEL STRENGTH

A plot of the maximum load for the HB210 and HB212 is shown in Figure 12. A t-test showed that there was a statistically significant ($p<0.05$) increase in t-peel strength due to autoclaving for the HB210.

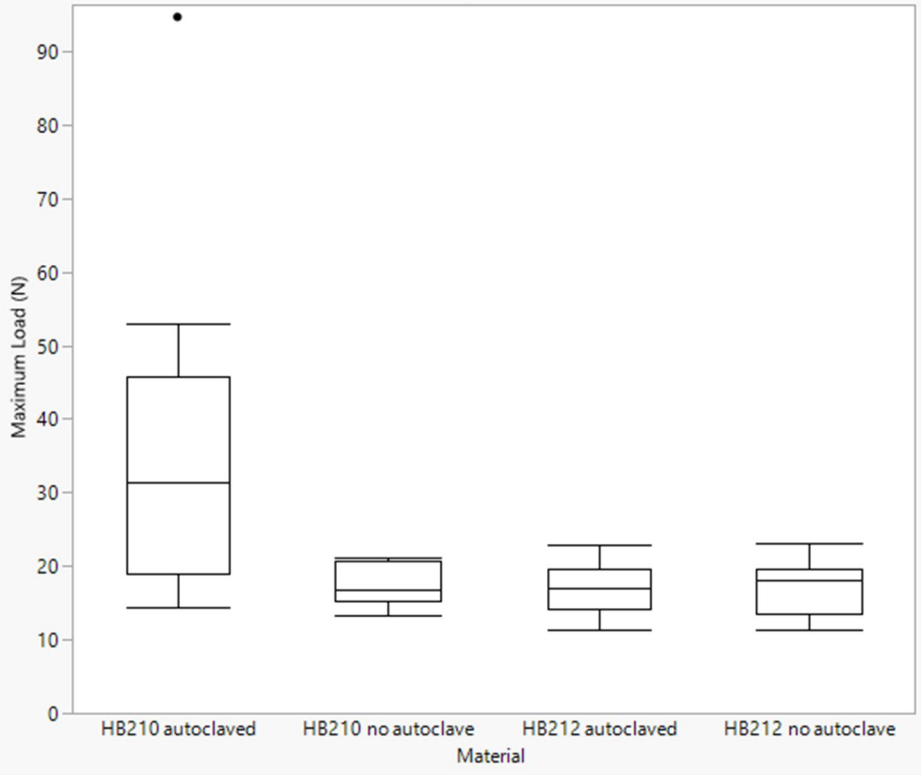

Figure 12 - Maximum load during a t-peel test of HB210 and HB212 before and after autoclaving

A representative extension vs load curve is shown in Figure 13. A higher load implies better adhesion between layers and could be attributed to increased melting and recrystallization upon cooling [23]. However, this was not observed in the DSC data shown later. Instead, it could be that the autoclaving process affects the transverse cohesive strength of the HB210 resin. Good adhesion is necessary for ensuring that the resin can transfer energy along the fibers, but if adhesion is too high it can prevent delamination from occurring which would decrease ballistic protection performance.

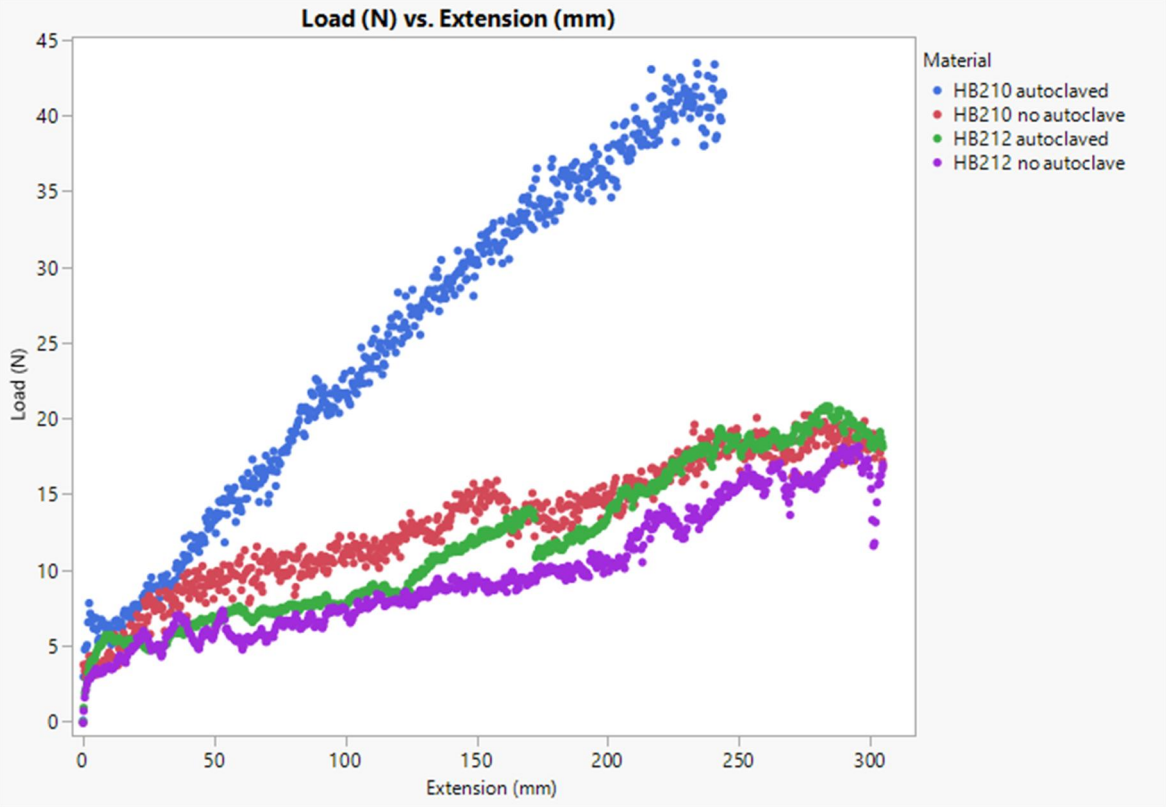

Figure 13 - Representative t-peel data for HB210 and HB212 before and after autoclaving

6.1.4 SHORT BEAM SHEAR STRENGTH

Short beam shear strength can be related to the inter-ply strength of the laminates. The failure mechanisms as shown in Figure 3 can offer insight into how the interlaminar properties affect ballistic performance. All samples exhibited interlaminar shear and inelastic deformation as shown in a representative sample of HB210 in Figure 14.

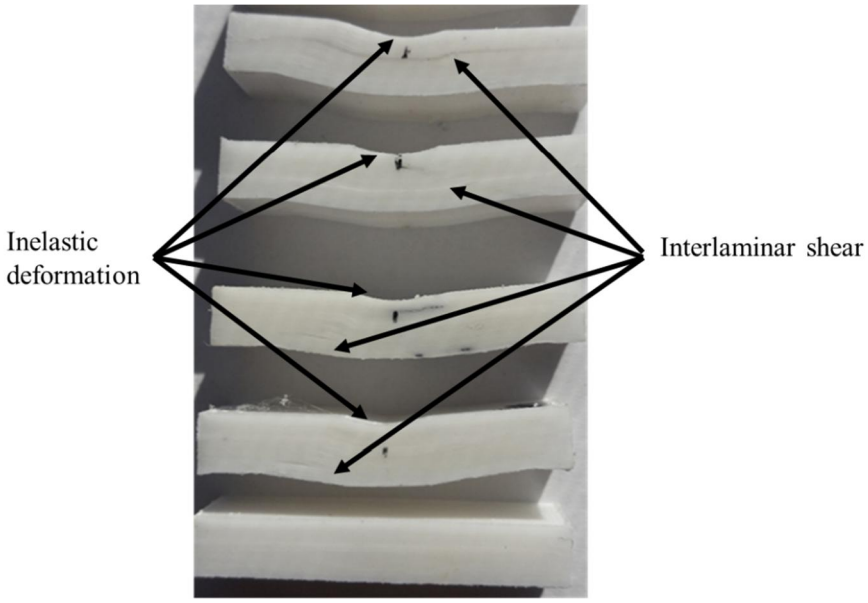

Figure 14 - HB210 after shear beam strength tests exhibiting interlaminar shear and inelastic deformation failure modes

A t-test showed that for HB210 there is a statistically significant ($p<0.5$) decrease in shear strength due to autoclaving as shown by the data in Figure 15. It could be that the additional pressure from autoclaving reduces the resin between crossing fibers which would make it easier for delamination to occur at those points, thus reducing shear strength. Another possibility that could explain the decrease in strength is the loss of crystallinity and molecular orientation due to excessive melting. This is in agreement with DSC results presented below. Additionally, the autoclave procedure may not be optimal for the HB210 polyurethane resin. The relatively low temperature and pressure settings may break some of the adhesive bonds during the softening step, but it not sufficient for the resin to flow and re-set.

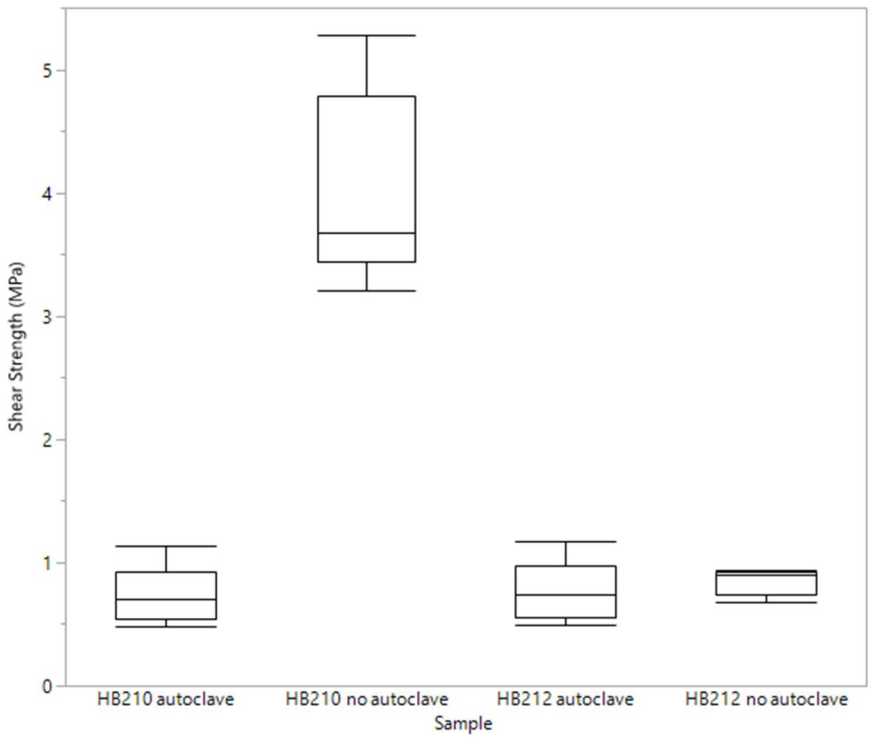

Figure 15 - Short beam shear strength of HB210 and HB212 before and after autoclaving

In materials with a lower shear strain, delamination will occur earlier in the impact event which can cause excessive back face deformation and structural bending in the armor. This prevents it from supporting the ceramic strike face of the armor, often leading to a decrease in ballistic performance.

6.1.5 FLEXURAL STRENGTH

Flexural strength as a measure of composite stiffness has been related to ballistic performance when the composite is paired with a strike face such as a ceramic [5, 9, 14]. The material must be stiff enough to provide good ceramic support but elastic enough to allow fibers to stretch to absorb energy from penetrating fragments after they pass through the ceramic.

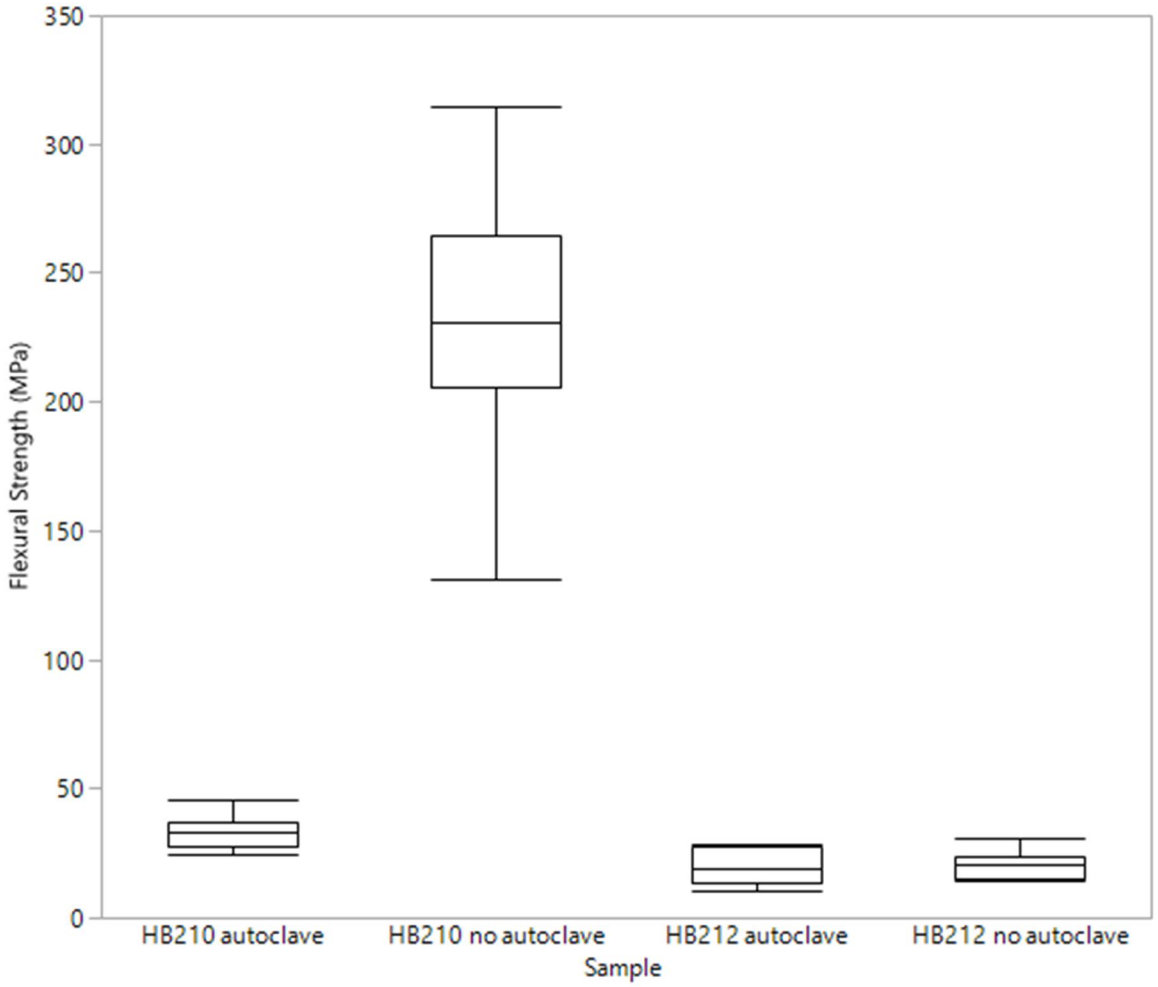

Figure 16 - Flexural strength of HB210 and HB212 before and after autoclaving

A t-test showed that for HB210 there was a statistically significant ($p<0.05$) decrease in flexural strength due to autoclaving as shown by the data presented in Figure 16. This is in agreement with the 3-point shear beam strength test.

The change in flexural and shear strength but preservation of tensile strength suggests that changes to the bulk properties due to fiber-resin interactions and resin type must be considered in addition to tensile strength when optimizing a composite for ballistic protection.

6.1.6 DSC

Thermograms are shown in Figures 17 and 18. Melting points, enthalpy, and crystallinity are summarized in Table 1 and were calculated using the methods described in Section 4.3.5.

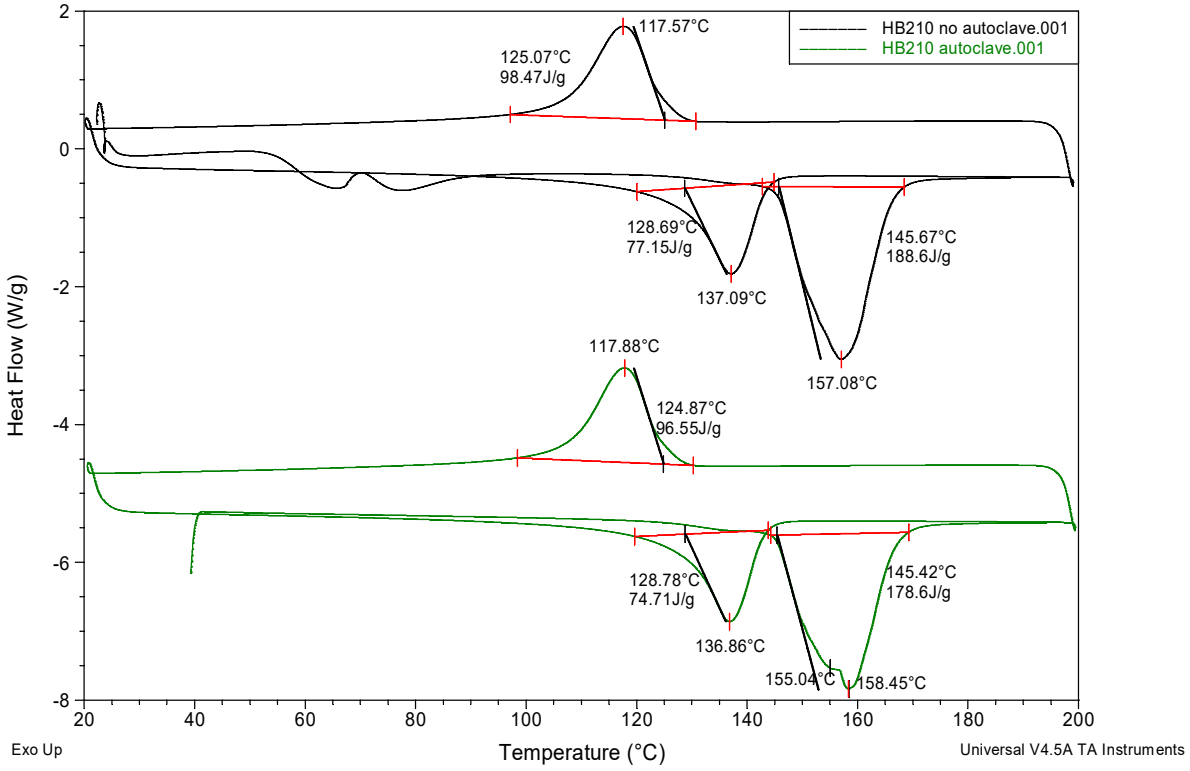

Figure 17 - DSC thermograms of HB210 before (black) and after (green) autoclaving

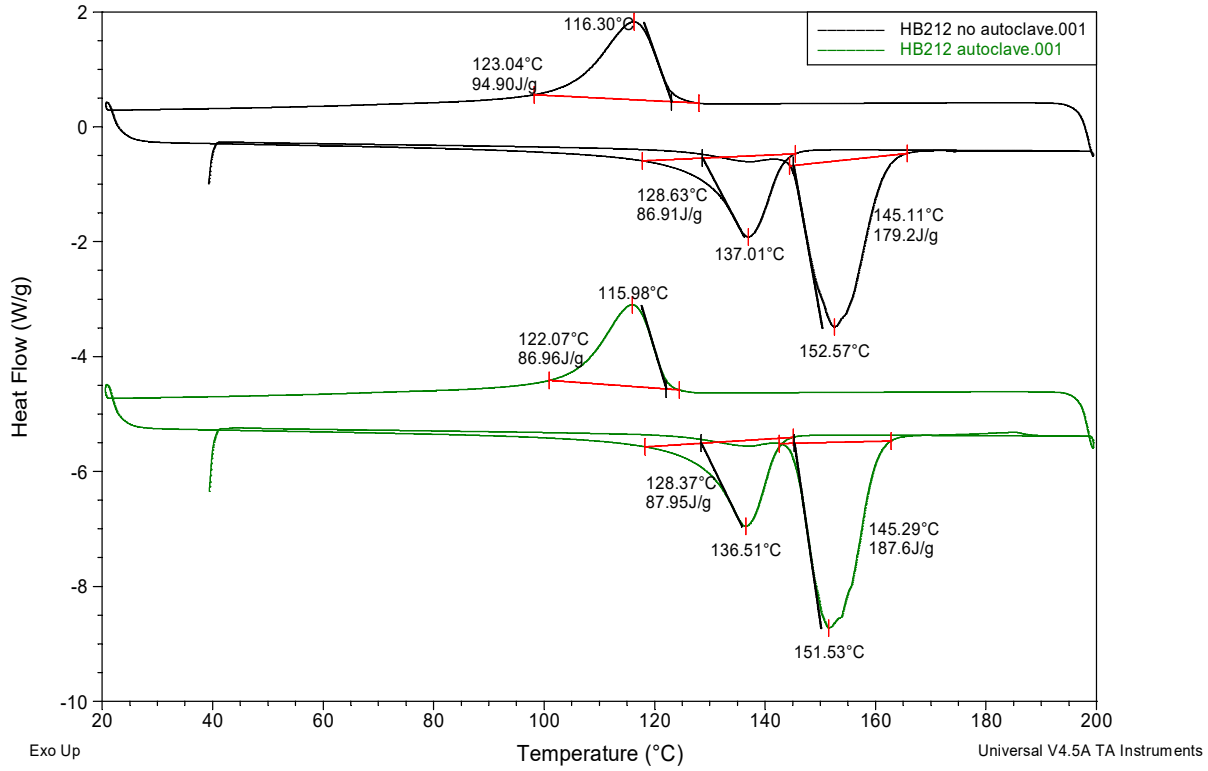

Figure 18 - DSC thermograms of HB212 before (black) and after (green) autoclaving

In the first heating cycle, the main melting peak occurs at roughly 145°C where the orthorhombic phase melts. The less pronounced melting peak at roughly 155°C correlates with the transformation of orthorhombic to hexagonal crystals in the UHMWPE [4, 6, 19]. The thermogram for HB210 after autoclaving shows an endotherm with a shoulder peak at 155.04°C and main peak at 158.45°C, which is the melting point of the hexagonal phase [19]. The melting temperatures during the second heating cycle at 136-137°C correspond to the melting of folded fins [1] and is in line with the melting temperature of unoriented PE [7]. HB210 saw a slight decrease in crystallinity from 64.4% to 61.0% during the first heating due to autoclaving, which may suggest some degradation and breakdown of the crystalline PE chains during the autoclaving process. The crystallinity of HB212 slightly increased when autoclaved, possibly due to the phenomenon of pressure-induced crystallization [12, 18].

Table 1 - Melting temperature, enthalpy, and percent crystallinity for HB210 and HB212 before and after autoclaving as determined by DSC

Sample	First Heat			Cooling		Second Heat		
	T_m (°C)	ΔH_m (J/g)	X_C (%)	T_c (°C)	ΔH_c (J/g)	T_m (°C)	ΔH_m (J/g)	X_C (%)
HB210, no autoclave	157.08	188.6	64.4%	117.57	98.47	137.09	77.15	26.3%
HB210, autoclaved	155.04, 158.45	178.6	61.0%	117.88	96.55	136.86	74.71	25.5%
HB212, no autoclave	152.57	179.2	61.2%	116.3	94.90	137.01	86.91	29.7%
HB212, autoclaved	151.53	187.6	64.0%	115.98	86.96	136.51	87.95	30.0%

As demonstrated by the tensile tests, this reduction in crystallinity did not negatively impact the tensile strength of the fibers. Heating beyond the onset of the melting peak at roughly 145°C would most likely show a negative impact on fiber strength. The thermograms also show a shallower, broad peak on the initial heating cycle at 140°C, with an onset of 125°C. This corresponds to the matrix melting. This data indicates that for autoclaving, the temperature should be slightly higher than 125°C to induce matrix flow but should not exceed the temperature at which the PE begins to melt.

6.1.7 BALLISTIC LIMIT, V_{50}

Flat plates with an areal density of 4.9 kg/m^2 were tested against 17 gr FSPs. The plates fronted with a ceramic were tested against the rifle round. The V_{50} was calculated using a regression curve of striking velocity vs response (penetration or partial penetration). Regression curves can be found in Appendices A and B.

A summary of 17 gr FSP V_{50} data can be found in Table 2. It has been shown from previous work [9] that FSP ballistic performance is a good indicator of rifle threat performance when the composite is combined with a ceramic. This is most likely because the ceramic deforms the projectile into a shape similar to that of a FSP. There was no significant difference in performance for HB210 before and after autoclaving. However, HB212 frag performance increased after autoclaving.

Table 2 - 17 gr FSP V_{50}s for HB210 and HB212 before and after autoclaving

	HB210	**HB212**
	V_{50} (m/s)	**V_{50} (m/s)**
NO AUTOCLAVE	672	627
AUTOCLAVE	648	721

Images of composites impacted with FSPs are shown in Figures 19 and 20. The autoclaved HB212 samples appear to undergo more extensive delamination and deformation than the pre-autoclave samples. This suggests that delamination may be an important factor energy absorption and can account for the increase in fragment protection in autoclaved HB212. No such change is visible in the HB210 samples.

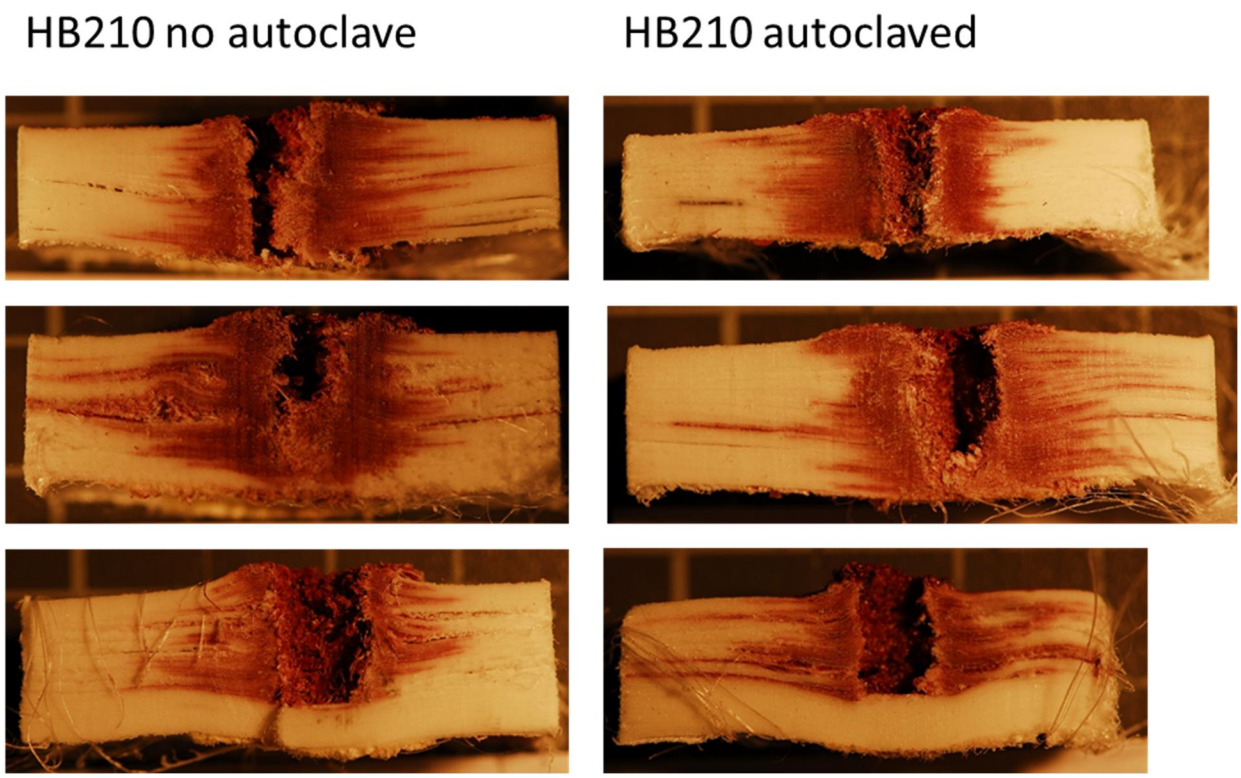

Figure 19 - Cross sections of HB210 impacted with 17 gr FSPs before and after autoclaving

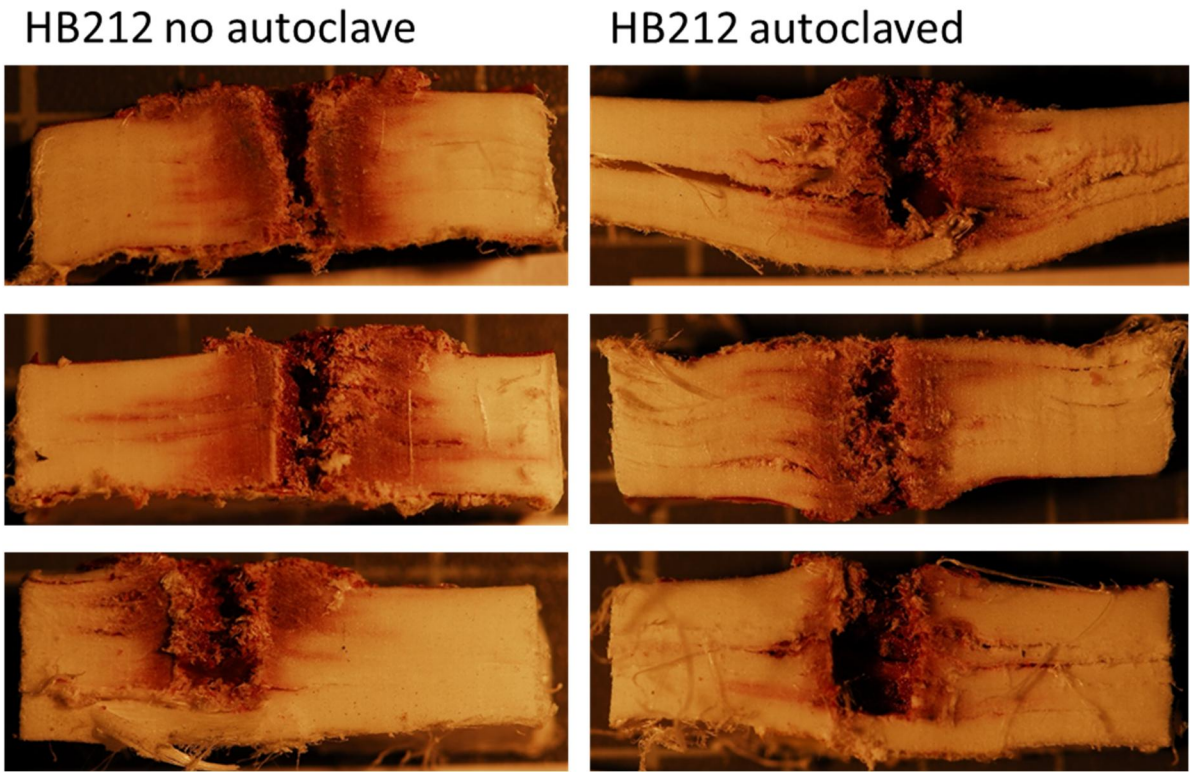

Figure 20 - Cross sections of HB212 impacted with 17 gr FSPs before and after autoclaving

Flat panels 19.05 cm x 19.05 cm in dimension with an areal density of 4.9 kg/m^2 were fronted with a CoorsTek® UltraSiC™ SC30 10.16 cm x 10.16 cm ceramic tile using Sikaflex®-252 and sent to NTS Chesapeake for testing against rifle rounds. A summary of the V_{50} values are shown in Table 3. The regression curves used to calculate the V_{50} can be found in Appendix B.

Table 3 - Rifle threat V_{50}s for HB210 and HB212 before and after autoclaving

	HB210	**HB212**
	V50 (m/s)	**V50 (m/s)**
NO AUTOCLAVE	983	968
AUTOCLAVE	990	971

When combined with the ceramic, there were no significant changes in ballistic performance against rifle rounds. This suggests that while autoclaving affects the properties of the composite, it did not affect the overall performance of the final ceramic-faced armor plate.

7 CONCLUSIONS AND RECOMMENDATIONS FOR FUTURE WORK

The polyurethane matrix of HB210 seemed to be most affected by autoclaving, possibly due to the nature of the resin. Autoclaving the stiff resin at relatively low temperatures and pressures may not allow it to flow very well and reset. Autoclave temperature, pressure, and dwell times were held constant for this work, but should be optimized for the resin systems of interest for future work. A stiffer polyurethane matrix may require a longer dwell time at high temperature to ensure it is softening enough to mold to the curved ceramic.

Only the HB212 with SIS triblock copolymer matrix saw an increase in frag protection, but when paired with a ceramic strike face there was no change in performance between autoclaved and non-autoclaved samples. It may be possible from this project to establish a relationship between the mechanical properties and frag protection for standalone composite-only plates or UHMWPE helmets.

It cannot be assumed from this work is that the rifle threat data applies for all ballistic threats. The use of a ceramic as a strike face also introduces many new variables when trying to establish a relationship between the composite properties and system-level armor performance. Any future design or modeling efforts require data on the hardening, strain rate sensitivity, and thermal softening of both the projectile and the target to have a full understanding of the system.

This effort validates DEVCOM SC's method of autoclaving curved SAPI samples during the R&D process. The process did not damage the tensile strength of the UHMWPE fibers, which is

the main contributor to ballistic performance. The significance is that the ability to use an autoclave without damaging the composite gives a wider selection of materials to choose from when it comes to using resins, adhesives, and reinforcements that cannot be air-cured. The autoclaving process also ensures good bonding between ceramic and composites which is important in good ballistic performance and energy transfer.

REFERENCES

1. “Honeywell Unveils Spectra Shield® 6166 for Increased Protection in Hard Body Armor.” Honeywell. Las Vegas, NV. Jan 21, 2020. Online: https://www.packagingcomposites-honeywell.com/spectra/press-releases/honeywell-unveils-spectra-shield-6166-for-increased-protection-in-hard-body-armor/

2. “Honeywell Launches Spectra Shield® 6472 for Improved Protection in Military Hemets.” Honeywell. Morris Plains, NJ. Oct 15, 2019. Online: https://www.packagingcomposites-honeywell.com/spectra/press-releases/honeywell-launches-spectra-shield-6472-for-improved-protection-in-military-helmets-2/

3. Lee, B.; Walsh, T.; Won, S.; Patts, H.; Song, J., and Mayer, A. “Penetration Failure Mechanisms of Armor-Grade Fiber Composites under Impact.” 2000.

4. Fejdys, M.; Landwijt, M.; Kucharska-Jastrzabek, A.; Struszcztk, M. The Effect of Processing Conditions on the Performance of UHMWPE-Fibre Reinforced Polymer Matrix Composites. FIBRES & TEXTILES in Eastern Europe (2016); 24, 4(118): 112-120

5. Karthikeyan, K.; Russell, B.; Fleck, N.; Wadley, H.; and Deshpande, V. The effect of shear strength on the ballistic response of laminated composite plates. European Journal of Mechanics A/Solids 42 (2013) 35-53.

6. Hsieh, A.; Chantawansri, T.; Hu, W.; Cain, J.; and Yu, J. New insight into the influence of molecular dynamics of matrix elastomers on ballistic impact deformation in UHMWPE composites. Polymer 95 (2016) 52-61

7. Xu, T. and Farris, R. “Shapeable Matrix-Free Spectra Fiber-Reinforced Polymeric Composites via High-Temperature High-Pressure Sintering: Process-Structure-Property Relationship” Journal of Polymer Science: Part B: Polymer Physics, Vol 43, 2767-2789 (2005)

8. Cunniff, P. “Dimensionless Parameters for Optimization of Textiles-Based Body Armor Systems.” 1999

9. O’Masta, Mark. “Mechanisms of Dynamic Deformation and Failure in Ultra-High Molecular Weight Polyethylene Fiber-Polymer Matrix Composites.” May 2014

10. Roth, M. Unpublished data. 2020.

11. O'Brien, D.; Parquette, B.; Bogetti, T.; Yiournas, A.; and Wagner, J. "High-Pressure Sintering of Ultrahigh Molecular Weight Polyethylene Film Laminates: Processing and Interlaminar Strength." ARL Technical Report ARL-TR-8105 (2017).

12. Masoomi, M.; Ghaffarian, S.; and Mohammadi, N. Influence of Matrix Type and Processing Conditions on the Morphology of the Interface and Interfacial Adhesion of PE/PE Composites. Proceedings of the Asian-Astralasian Conference on Composite Materials, Sydney, Australia, (ACCM-4), 2004.

13. Xu, Tao and Farris, Richard. "Optimizing the Impact Resistance of Matrix-Free Spectra Fiber-reinforced Composites." Journal of Composite Materials, ¬Vol. 39, No 13 (2005) 1203-1220.

14. Xu, T. and Farris, R. "Shapeable Matrix-Free Spectra Fiber-Reinforced Polymeric Composites via High-Temperature High-Pressure Sintering: Process-Structure-Property Relationship" Journal of Polymer Science: Part B: Polymer Physics, Vol 43, 2767-2789 (2005)

15. Kartikeya, K.; Chouhan, H.; Ahmed, A.; and Bhatnagar, N. "Determination of tensile strength of UHMWPE fiber-reinforced polymer composites." Polymer Testing 82 (2020).

16. Karthikeyan, K. and Russell, BP. "Polyethylene ballistic laminates: Failure mechanics and interface effect." Materials and Design 63 (2014) 115-125.

17. Ghiorse, S., Horwath, E., Montgomery, J., and Hoppel, C. "Effect of Backing Plate Properties on the Ballistic Response of Ceramic-Based Structural Armor." ARL-RP-56. Sept. 2002.

18. Hazell, Paul J. "Armour: Materials, Theory, and Design." CRC Press 2016.

19. Taylor, SA and Carr, DJ. "Post failure analysis of 0°/90° ultra high molecular weight polyethylene composite after ballistic testing." Journal of Microscopy Vol 196 (1999) 249-256.

20. Ramuni, V.; Yuan, Q.; Chen, J.; and Misra, R.D.K. "Pressure-induced crystallization of polymers with dispersion of nanoparticles: Structure, interfacial interaction, and micromechanism of fracture." Materials Science and Engineering A 527 (2010) 4281-4299.

21. Zherebtsov, D., Chukov, D., Torokhov, V., Statnik, E. “Manufacturing of Single-Polymer Materials Based on Ultra-high Molecular Weight Polyethylene Fibers by Hot Compaction.” Journal of Materials Engineering and Performance. 2020.

22. Koushyar, Hoda. “Effects of Variation in Autoclave Pressure, Cure Temperature, and Vacuum-Application Time on the Porosity and Mechanical Properties of a Carbon/Epoxy Composite.” Wichita State University 2007.

23. Xu, T. and Farris, R. “Optimizing the Impact Resistance of Matrix-free Spectra Fiber-reinforced Composites.” Journal of Composite Materials (2005) Vol. 39 No. 13

24. Cain, J.; Vargas-Gonzalez, L.; and Gaviola, M. “A Quasi-Static Indentation Methodology for Screening Ultra-High Molecular Weight Polyethylene Composites for Ballistic Performance,” (2018) Technical Report ARL-TR-8457

25. Helliker, A. Lightweight Ballistic Composites 2nd Ed. Woodhead Publishing Series in Composites Science and Engineering 2016.

26. Zhang, X.; Wang, Y.; Lu, C., Cheng, S. “Interfacial adhesion study on UHMWPE fiber-reinforced composites.” Polymer Bull. (2011) 67:527-540.

27. ASTM Standard D2344M-13, 2013, “Standard Test Method for Short-Beam Strength of Polymer Matrix Composite Materials and Their Laminates,” ASTM International, West Conshohocken, PA.

28. Lassig, T., May, M., Heisserer, U. et al. “Effect of consolidation pressure on the impact behavior of UHMWPE composites.” Composites Part B: Engineering. Vol 47, pp 47-55. 2018.

29. ASTM Standard D1876, 2008, “Standard Test Method for Peel Resistance of Adhesives (T-Peel Test),” ASTM International, West Conshohocken, PA.

30. ASTM Standard D7264, 2015, “Standard Test Method for Flexural Properties of Polymer Matrix Composite Materials,” ASTM International, West Conshohocken, PA.

31. ASTM Standard D792-13, 2013, “Standard Test Methods for Density and Specific Gravity (Relative Density) of Plastics by Displacement,” ASTM International, West Conshohocken, PA.

APPENDIX A – 17 GR FSP BALLISTIC REGRESSION CURVES

HB210 no autoclave

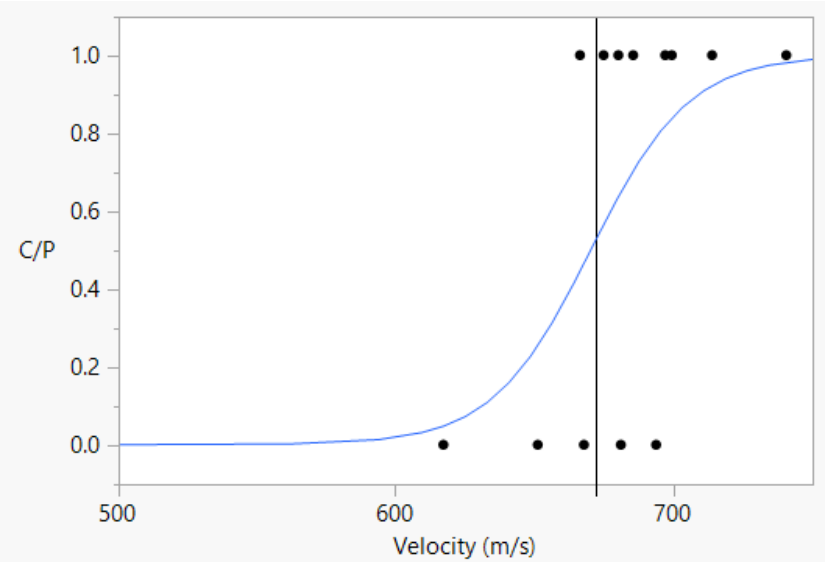

HB210 autoclaved

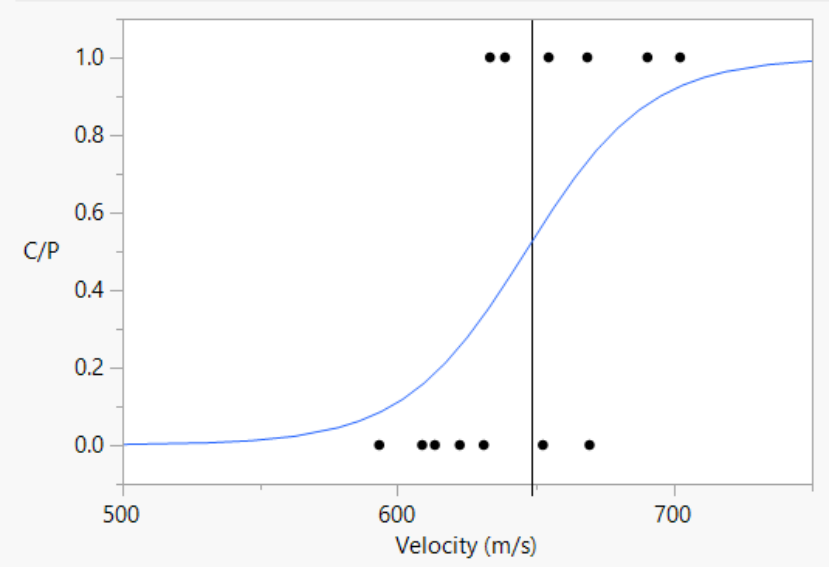

HB212 no autoclave

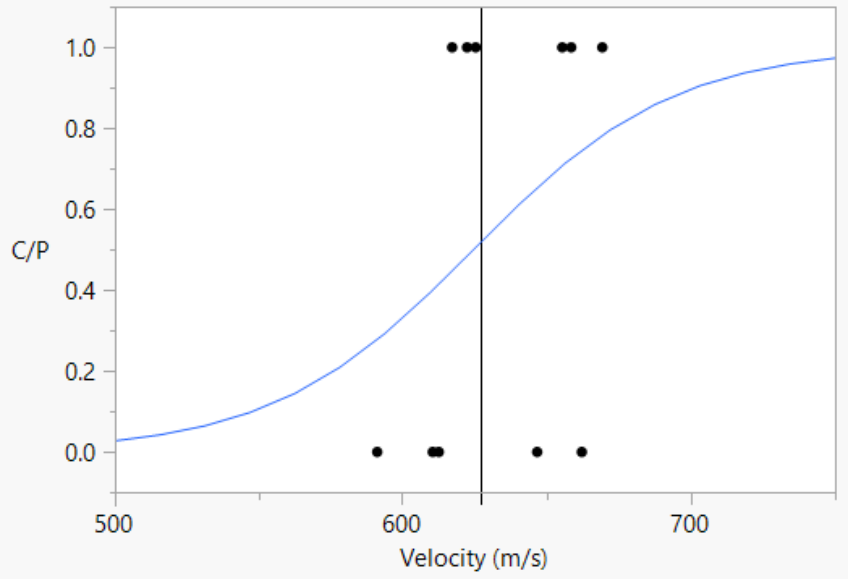

HB212 autoclaved

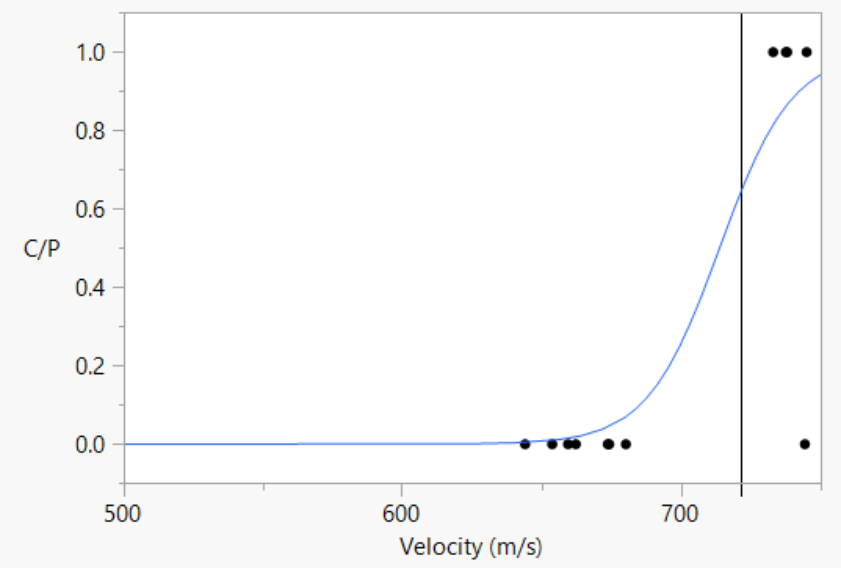

APPENDIX B – RIFLE THREAT REGRESSION CURVES

HB210 no autoclave

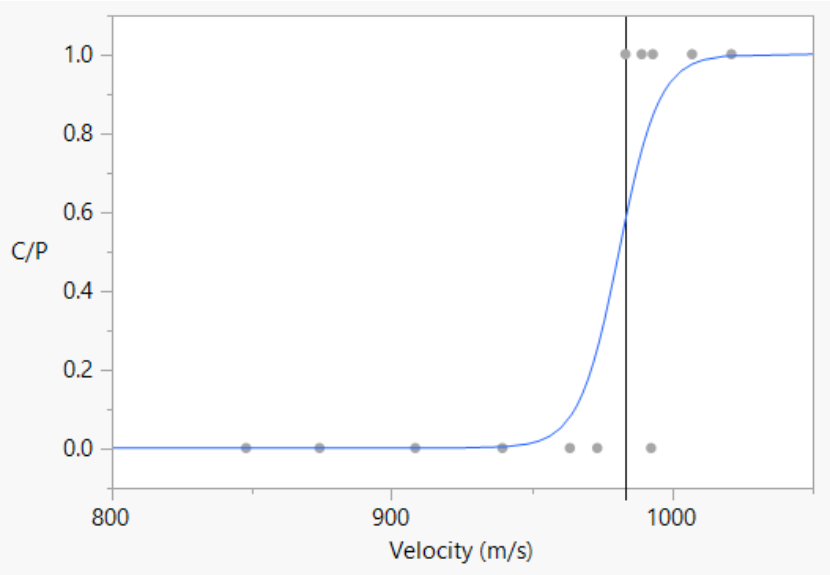

HB210 autoclaved

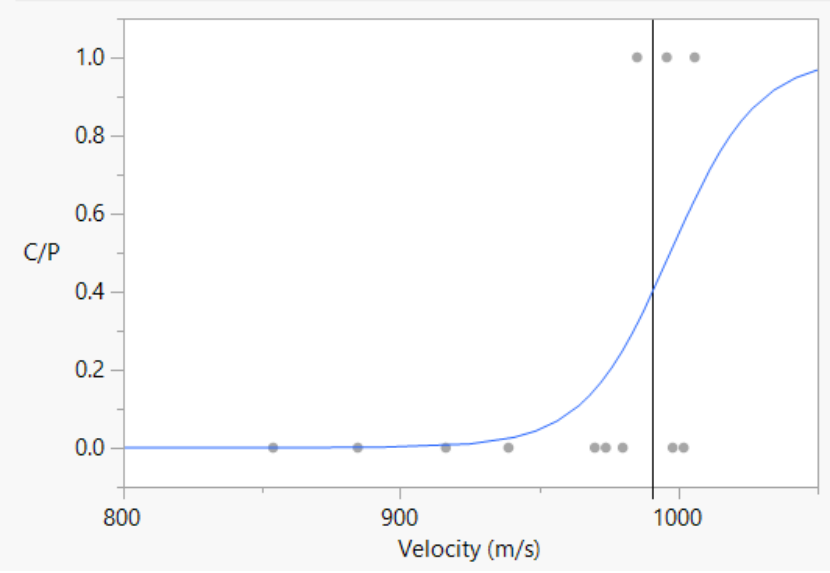

HB212 no autoclave

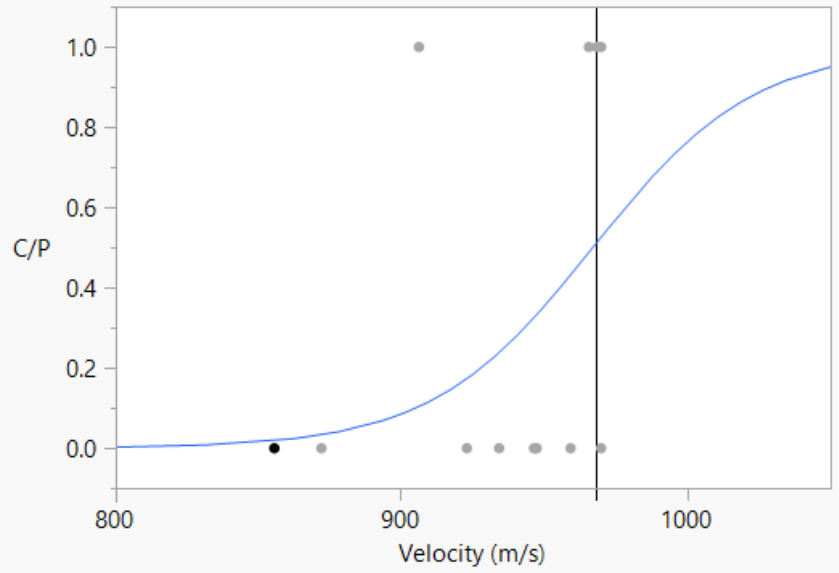

HB212 autoclaved